Journal of Fluorescence
https://doi.org/10.1007/s10895-023-03443-5

RESEARCH

Construct Fluorescent Solid Lipid Nanoparticles from Bacterial Outer Membrane Vesicles to Study their Properties and Potential Applications as In Vivo and Invitro Imaging Agents

Viswanathan kaliyaperumal[1] · Vimal Manivannan[2] · Chitra Karuppanan[2] · Dhinakar Raj Gopal[3] · Raman Muthusamy[4]

Received: 17 August 2023 / Accepted: 16 September 2023
© The Author(s), under exclusive licence to Springer Science+Business Media, LLC, part of Springer Nature 2023

Abstract
In this study, the new solid lipid nanoparticles were created by combining fluorescent dye, fatty acid, lipid, and bacterial outer membranes. The synthesised particles were roughly 95–100 nm in size. Vero cells cultivated with these nanoparticles showed no cytotoxicity in 5-dimethylthiazol-2-yl-2, 5-diphenyltetrazolium bromide (MTT) assay. In the cell uptake studies, the vero cell line was employed. Cell lines absorbed fluorescent solid lipid nanoparticles (FSL NPs) better, according to the findings. The confocal microscopy results revealed a significant accumulation of FSL NPs in the cytoplasm over time. The results of small animal imaging employing BALB/c mice revealed that the nanoparticles generated provided high contrast signals. Overall, the OMVs-based FSL NPs system offers a unique imaging tool for studying intracellular interactions as well as a viable tool for drug delivery.

Keywords Fluorescent solid lipid nanoparticles · Rhodamine · Fluorescent nanoparticles · Imaging

Introduction

Natural tri glycerides and their derivatives were used to create solid lipid nanoparticles (SLN) [1, 2]. SLN nanoparticles are well suited for pharmaceutical applications such as medicine administration, vaccine delivery, and cosmetic cream formulations [3, 4]. The physical characteristics of the SLN nanoparticles varied depending on the synthesis procedure. Several groups reported high pressure homogenization approach based SLN Nanoparticles using hot and cold temperatures, and this method yielded a significant amount of SLN nanoparticles [5]. Solvent emulsification [6], solvent diffusion [7, 8], and high speed homogenization [9] are examples of wet lab techniques. The main advantage of solid lipid nanoparticles is their high drug loading percentage, as well as their minimal water dispersion and drug release. The SLN nanoparticles are biocompatible and can be used in biological applications. Red blood cell membrane [9], leukocyte membrane [10], and cancer cell membrane coated nanoparticles have previously been reported [11]. Bacterial membranes include a variety of immunogenic antigens that promote adaptive immune responses [12, 13]. The combination of bacterial outer membrane protein, fatty acid, and glycerol resulted in the development of new biomimic materials. The incorporation of solid lipid compounds into bacterial membranes will aid in the protection of the membranes' biological properties. The solid lipid materials also provided custom-designed particles of varying size and shape, as well as various surface functional groups. The fluorescent probe precisely connected target specific marker was employed for particular targeting and visualisation [14, 15]. Various functional fluorescent materials have been used in biological science for bio imaging applications. Small organic dyes

✉ Viswanathan kaliyaperumal
viswanathanphd@yahoo.com

1 Department of Chemistry, Saveetha School of Engineering, Saveetha Institute of Medical and Technical Sciences (SIMATS), Chennai 600077, India

2 Translational Research Platform for Veterinary Biologicals, Centre for Animal Health Studies (CAHS), Tamil Nadu Veterinary and Animal Sciences University (TANUVAS), Chennai 600051, India

3 Department of Biotechnology, Madras Veterinary College, Tamil Nadu Veterinary and Animal Sciences University (TANUVAS), Chennai 600051, India

4 Department of Microbiology, Centre for Infectious Diseases, Saveetha Dental College and Hospitals, Saveetha Institute of Medical and Technical Sciences (SIMATS), Chennai 600077, India

Published online: 25 September 2023

(600–900 nm) are commonly employed in bio imaging, however they have certain drawbacks in in vivo applications, such as poor solubility and low luminous quantum yield [16, 17]. The use of organic dyes in the nanotechnology allowed for the flexible fabrication of the bio probe for in vitro and in vivo applications. The fluorescent dye encapsulated nanomaterials were created using dye encapsulation, dye adsorption, or grafting [18]. Typically, two types of nano fluorescent probes were reported, such as organic and organic nano probes. Organic dyes are currently being used to generate near infrared imaging nano probes [19–21]. Previously, fluorescent solid lipid nanoparticles for tumour imaging were described because the lipid nanoparticles showed substantial affinity for overexpressed lipoprotein receptors in breast and prostate malignancies [22]. Solid lipid nanoparticles are likewise attracted to lymphatic channels and lymph nodes. The cytotoxicity of the solid lipid nanoparticles was extremely low. Based on the benefits listed above, solid lipid nanoparticles favour the development of dye-loaded nanostructures for clinical imaging [23, 24]. In this study, we used a simple emulsion-solvent evaporation approach to create new fluorescent solid lipid nanoparticles. To make the nanoparticles, the bacterial outer membrane protein was separated using the deoxy cholate extraction process and then covered by a solid lipid layer made of cholesterol, Glyceryl mono-stearate, and soya lecithin, as well as conjugated with rhodamine isocyanides. The cytotoxicity of the synthesised nanoparticles was investigated using the MTT assay, and cell imaging experiments were carried out utilising vero cell lines. FACS was used to examine cell uptake at various time intervals. BALB/c mice were used for the small animal imaging.

Materials and Method

Isolation of Bacterial Outer Membrane from *Escherichia coli (E.Coli)*

The *E.Coli* were grown in Tryptone Soya Broth overnight before being extracted by centrifugation at 5000 rpm for 10 min and suspended in sodium chloride buffer. The cell suspension was maintained at Gel Rocker for 30 min, and the total wet weight of the suspension was calculated. The cell suspension was centrifuged for 60 min at 2900 g, and the pellet was suspended in 0.1 M Tris-10 mM EDTA buffer at a 7.5:1 wet weight ratio. The outer membrane protein was extracted by adding 1/20th volume of 0.1 M Tris, 10 mM EDTA, and 10% deoxycholate (DOC), and the membrane was separated from cell debris at 20000 g for 1 h at 4 °C. The supernatant containing the outer membrane protein was ultracentrifuged at 125000 g for 2 h at 4 °C. The pellet was resuspended in 0.1 M Tris, 10 Mm EDTA, 0.5% DOC buffer, and the solution was centrifuged at 125000 g for 2 h at 4 °C. The concentrated outer membrane was resuspended in a solution of 3% sucrose. The samples obtained after each centrifugation during the Deoxycholate Extraction technique of bacterial outer membrane isolation were kept and loaded in SDS—PAGE. Protein separation was accomplished using the protein's molecular weight. The final outer membrane pellet resuspended in sucrose was placed in the last lane, followed by a pre dyed ladder, and the outer membrane's molecular weight was determined to be 60–65 Kda. The total protein was calculated using the BCA Protein Assay Kit according to the kit instructions, and the protein was assessed to be 0.125 mg/ml.

Preparation of Fluorescent Solid Lipid Nanoparticles (FSL NPs)

To create the nanoparticles, 88 ml of isovaleric acid (IVA) was mixed with 10 ml of water and allowed to dehydrate. To create an emulsion, the IVA—water mixer was combined with taurodeoxycholic acid sodium salt (500 mg), lecithin (500 mg), cholesterol (1 g), 1 mL of bacterial outer membrane, and 0.2 mL of trimethylamine. For the fluorescent, the required amount of rhodamine isocyanide was added, and the emulsion was ultrasonically emulsified before the solvent was evaporated using hot air alone and freeze dried at −48 °C.

Cell imaging with Confocal Microscopy

Vero cells cultivated in DMEM media were grown in cover slips until 60% confluent. The cells were treated with fluorescent solid lipid nanoparticles for 0.5, 2, and 4 h. The stained cells were imaged using a Carl Zeiss LSM 700 laser scanning confocal microscope with a 63 objective. Image J software was used to do the quantitative evaluation.

In Vivo Imaging Using BALB/c Mice

All in vivo studies were carried out in accordance with the instructions of the TANUVAS Ethical Committee, IAEC approval No.2172/ DFBS/2018 in Chennai. The nanoparticles were administered intraperitoneally to anaesthetized animals and observed after 30 min. The fluorescence intensities in the live animal system were measured using the IVIS Lumina LT series III (Calliper, MA). During imaging, the proper rhodamine excitation and emission filters were utilised, and background signal was removed from two-dimensional images before image scaling was normalised by converting total radiance efficiency. The intensity of fluorescence was expressed by a multicolor scale ranging from blue (least intense) to red (most intense). For anatomical renderings, signal intensity pictures were placed on full

scale reference photographs. To normalise the intensity of the fluorescence across time points, scales were manually set to the same levels for comparable photographs. The intensity of fluorescence inside particular parts of individual animals was assessed using the region of interest (ROI) capabilities in the PerkinElmer Live Image 4.5 software. The in vivo transmission of fluorescent intensity was investigated using PerkinElmer live imaging software.

Cell Uptake Studies Using FACS

The uptake of solid lipid nanoparticles was studied using a Flowcytometry Beckman Counter Fluroscence Activator Cell Sorter (FACS) Moflo XDP. Fluorescence was stimulated at 525 nm, and emission at 545 nm was captured continuously at an analysis rate of 100–200 cells per second, as well as forward and side scatter. Nanoparticles were treated with 1 ml of cells for 0.5, 2, and 4 h before being examined with a flow cytometer. The nanoparticle uptake experiments began with the measurement of nanoparticle autofluorescence. The temporary increase in sample pressure cleared particles from the tubing. Data collecting continued for another 10 min. The mean relative fluorescence intensity was calculated using the submit programme after eliminating debris signals by establishing appropriate gates in the forward and side scatter histograms, and the initial stained cells were visualised within 10 s. The peak shift of the histogram is readily visible in the submit programme, and the differences in the histograms of each figure represent cell uptake over time.

Blood Biocompatibility Assay

Based on a previous publication [25], the blood biocompatibility was investigated using mice blood. In brief, the whole blood haemolysis experiment was carried out using produced FSLP NPs. The blood was drawn in vacutainers containing 24 IU sodium heparin (Becton Dickinson, Inc., USA). A volume of 200 µL uncoagulated whole blood was taken and combined with 50 µL of various concentrations of FSLP nanoparticles. Following addition, the samples were gently mixed and incubated at 37 °C for 4 h. The samples were then centrifuged at 1200 rpm for 10 min to get the plasma. The plasma was then centrifuged at 13,000 rpm for 15 min to remove the nanoparticles, and the supernatant was analyzed for the presence of haemoglobin using a particular 545 nm spectrophotometric absorption. A 2% Triton-X 100 was used as positive control and normal saline as the negative control. The red blood cell haemolysis assay was performed after the mice RBC were separated by centrifugation. 200µL of RBC was combined with 50µL of FSLP NPS in varied concentrations. The mixture was incubated at 37 °C for 2 h before being centrifuged at 1500 rpm for 5 min to check for released haemoglobin at 545 nm. As a positive control, 2% Triton-X100 was employed, and normal saline was used as a negative control. The percentage of haemolysis was estimated using a relative technique based on the optical density (OD) measurements as follows:

$$\% \text{ of haemolysis} = (\text{OD sample} - \text{OD negative}) / (\text{OD positive} - \text{OD negative}) \times 100$$

The RBC cells were collected as described above, mixed with FSLP nanoparticles at varied concentrations, and incubated for 30 min at 37 degrees Celsius. The RBC aggregation was discovered on a phase contrast microscope at a magnification of 40×.

Results and Discussion

The solvent evaporation approach was utilised to make solid lipid nanoparticles. Biodegradable particles are extremely important in medicine delivery and targeted applications. The lipids were first dissolved in solvent before being combined with fluorescent and bacterial outer membranes. The bacterial outer membrane was first isolated using the deoxycholate (DOC) extraction method. SDS-PAGE was used to establish the purity of the extraction and its molecular weight, as shown in Fig. 1a. The isolated outer membrane protein exhibited a band of around 60–65 KDa, and the protein concentration was measured using a BCA assay kit to be approximately 125 µg/mL. The particle size was determined using a particle size analyzer and transmission electron microscopy (TEM), as illustrated in Fig. 1b. It found that the solid lipid nanoparticles ranged in size from 95 to 100 nm. The fluorescence life duration was measured with an excitation wave length of 535 nm. Approximately 100 nanoparticles were collected, and the principal component decay was 30 ns, while the individual particle intensity remained greater than 600 ns and no blinking was detected up to 1 ms, as shown in Fig. 1c. Figure 1d depicts photographs of fluorescent solid lipid nanoparticles and their emission and absorption spectra. The MTT reagent was used to investigate the toxicity of the solid lipid nanoparticles, and the results are presented in Fig. 2. The results showed that up to 250 mg/ml caused no significant toxicity, but 500 mg/ml caused 10% toxicity. As a result, the foregoing investigations concluded that a concentration of 250 mg/ml solid lipid nanoparticles is ideal for distribution applications. During synthesis, electrostatic interaction between OMV and lecithin molecules modified the composition of the OMV. Lecithin interacts with proteins and polysaccharides in OMV, causing surface modifications. This interaction also reduces their innate complexity and the overall net charges were changed to avoid aggregation and FSLP also consists of lipophilic compound along with protein it will reduce aggregation with blood cells and it was confirmed by performing the aggregation test against mouse blood and the results were added

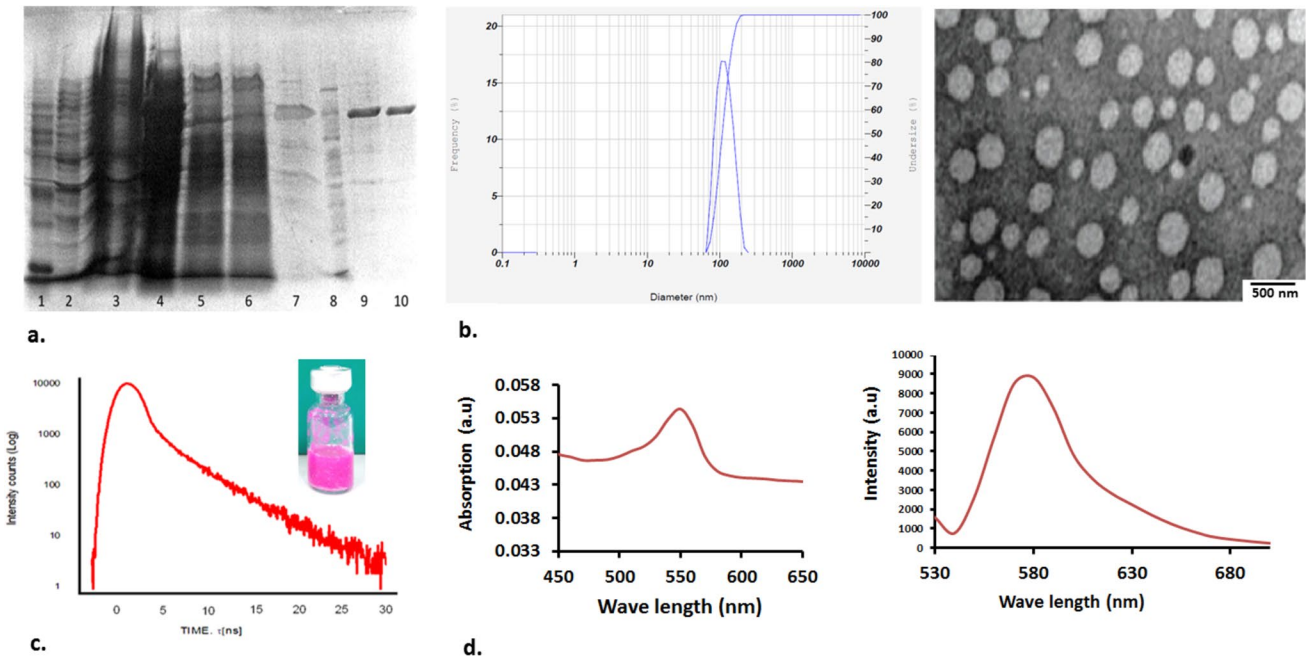

Fig. 1 **1a** Confirmation of bacterial outer membrane purification using SDS − PAGE: The samples collected as supernatant after centrifugation were in lanes 1, 3, 5, and 7. Lanes 2, 4, 6, 9, and 10 included the pellet samples taken after each centrifugation. Lane 8 is a protein marker that has been stained. **1b** DLS studies of fluorescent solid lipid nanoparticles in milli-Q-water revealed an average size of 100 nm. Images of solid lipid nanoparticles taken using a transmission electron microscope (TEM). **1c** The results of fluorescent solid lipid NPs' lifetime measurements. According to the exponential decay, the NPs had a 3% quick component and a 97% slow component. **1d** A multi plate reader was used to record the absorption and emission spectra. Wavelength of excitation (λ = 545 nm)

to Supplementary materials Fig. 2. The whole blood haemolysis results in 2a. suggested that nanoparticles concentration-based haemolysis occurred. The particle concentration up to 250 mg/ml causes only 4.65% of haemolysis, while the highest concentration of 500 mg/ml causes maximum 7.56% of haemolysis, and haemolysis percentages less than 10% are deemed non-toxic. The erythrocyte haemolysis was assessed by haemoglobin measurement. The toxicity of FSLNPs causes membrane lysis and haemoglobin release. Figure 2a. shows that 500 mg/ml causes less than 10% haemolysis. The aggregation was tested to evaluate the impacts of FSLP nanoparticles aggregation effects on RBC, and the cell was observed under a microscope as shown in Fig. 2b. The results showed that there are no aggregations up to 500 mg/ml, which was confirmed by a microscope. The fluorescent solid lipid nanoparticles generated were used as an imaging tool for the vero cell line. Vero cells were chosen in this investigation because NPs toxicity will directly affect the cytoplasm and cause it to become granules, as well as the cellular contents to become aggregation and accumulate on one side of the cells, which can be easily spotted using an inverted microscope. As a result, vero cells were chosen for uptake investigations. For this study, red fluorescence was photographed with a confocal microscope, and the nucleus was labelled with DAPI and emitted blue light. The uptake of nanoparticles was examined at different time intervals (0.5, 2, and 4 h), as shown in Fig. 3. The localised emission spectra from the vero cells show the characteristic peak at 545 nm, and the autofluorescence is completely erased. The red fluorescence caused by the solid lipid nanoparticles was noticed in the cytoplasm of the exposed vero cell using confocal microscopy. Due to particle size and the

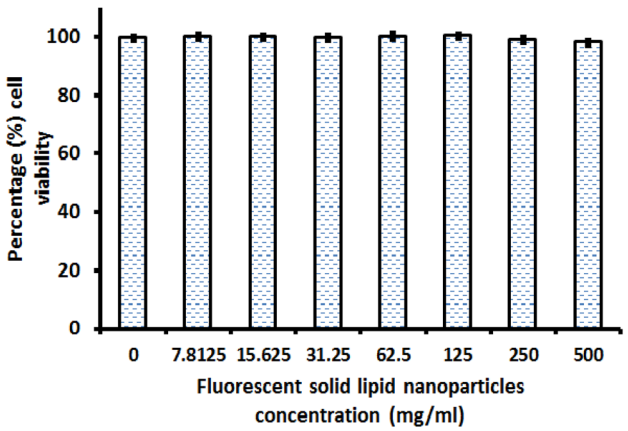

Fig. 2 MTT assay-based cell cytotoxicity study results of fluorescent solid lipid nanoparticles in vitro (S.D = 3%, n = 3)

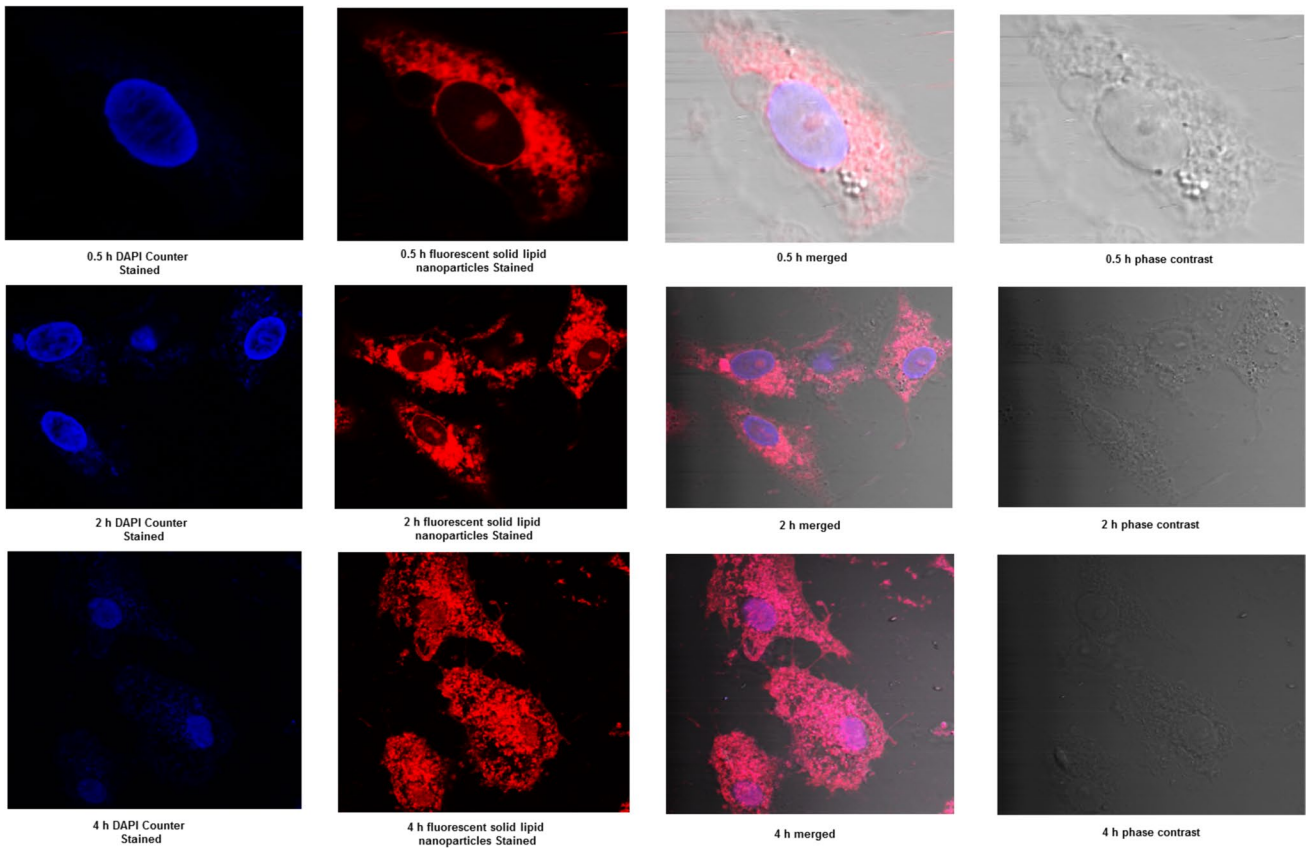

Fig. 3 Confocal microscopy photos of vero cells incubated with fluorescent solid lipid nanoparticles for 0.5 4 h at 37 °C with 125 µg/mL fluorescent solid lipid nanoparticles, exhibiting particle cellular uptake and intracellular localisation. Scale bars are 50 m long

fatty acid included in the FSL NPs, 60% of the NPs collect on the cytoplasm after 2 h, and nearly 90 percent of the particles reach the nucleus after 4 h. After the cells were extracted from the media, the cell fluorescence intensity of the solid lipid nanoparticles was estimated and quantified using a multi plate reader. The cell imaging and fluorescence quantification revealed that the vast numbers of nanoparticles were taken up after 30 min and that the nanoparticles were not affected or aggregated by serum. In this preliminary research, the organic dye was combined with solid lipid nanoparticles to investigate the efficacy of the delivery carrier and its transport path. The vero cell line-based nanoparticle uptake investigations verified that the particles enter the cell nucleus via passive diffusion through the nuclear pore complex formation due to their relatively small size. Furthermore, the flow cytometer-based analysis results showed a significantly higher uptake of solid lipid nanoparticles within 30 min, and we discovered no time-dependent increase in cell-associated fluorescence of solid lipid nanoparticles in cell lines as seen from the comparison of fluorescence at the three time points (Fig. 4). BALB/c mice were used to test the invivo imaging suitability of the solid lipid nanoparticles. The mouse was given intraperitoneal injections of fluorescent solid lipid nanoparticles (0.7 ng/kg) in three separate body locations. The mouse was photographed after post-injection using an IVIS Lumina LT series III imaging system (Calliper, MA), and the results are displayed in Fig. 5. The results showed that fluorescent solid lipid nanoparticles are extremely appropriate for imaging, producing bright luminous and detectable particle signals. It is crucial to highlight that no signs of toxicity were found in the mice that were injected with the solid lipid nanoparticle; they appeared to be healthy following the injection. The use of isovaleric acid as a solvent to dissolve OMV, lecithin, and cholesterol was reported for the first time. The evaporation took place at a low temperature, which allowed for the easy inclusion of organic colours. Isovaleric acid also promotes the formation of monodisperse nanoparticle suspensions. Easy to freeze dry to eliminate extra emulsions. The approach is extremely simple and well suited for lab-scale synthesis of solid lipid nanoparticles. The OMV-based fluorescent solid lipid nanoparticles demonstrated various advantages, including the phospholipid bilayer of OMV, which allows for facile incorporation, modifications with lecithin, cholesterol, and fatty acid. The OMV demonstrated a high ratio of binding with lecithin and cholesterol, which protects the protein layer and allows the particles to circulate for a longer period of time. The described approach demonstrated the controlled production of FSLNPs with sizes ranging from

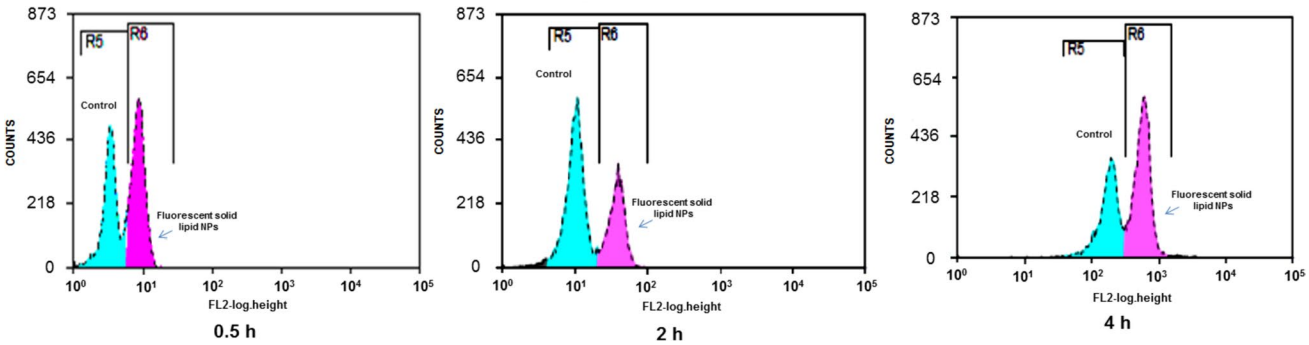

Fig. 4 Flow cytometry was used to measure cell absorption of fluorescent solid lipid nanoparticles. The cells were treated with 100 mg/ml nanoparticles for 0.5, 2 and 4 h. FACS was used to measure the fluorescence

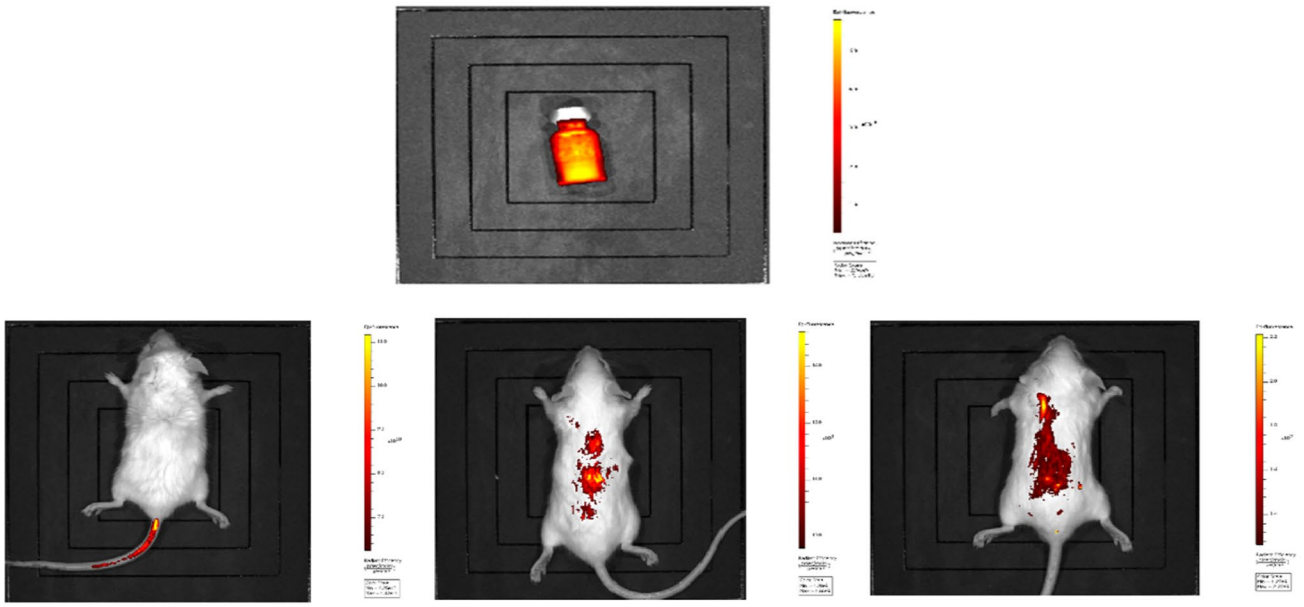

Fig. 5 Whole-animal imaging using BALB/C mice. Fluorescent solid lipid nanoparticles were delivered into the mouse. The mouse was photographed in three different positions: tail, back, and in the centre of the body

90 to 100 nm. The FSL NPs that have been produced are excellent alternative carriers for therapeutic peptides, proteins, and antigens. This study indicates that FSL NPs meet the parameters for a therapeutic particle carrier system that can be supplied via parenteral routes or alternate routes such as oral, nasal, and pulmonary. The use of FSL NPs improves protein stability, prevents proteolytic degradation, and allows for the prolonged release of integrated molecules.

Conclusion

Finally, fluorescent solid lipid nanoparticles with high fluorescence properties were effectively generated utilising an evaporation approach. The outer membrane vesicle of *E.Coli* was successfully extracted and integrated with fat and lipid molecules using a mix of emulsion and evaporation methods, and the properties of the nanoparticles were successfully examined. The toxicity and compatibility experiments revealed that the solid lipid nanoparticles are extremely biocompatible due to their composition. The utility were further extended as an imaging tool to explore cell localization and in vivo imaging, and the results demonstrated that the particles are well suited for cell tracking, drug administration, and labelling applications.

Supplementary Information The online version contains supplementary material available at https://doi.org/10.1007/s10895-023-03443-5.

Authors' Contributions Viswanathan kaliyaperumal – Complete manuscript writing, experimental design, and physicochemical

characterisation of FSL NPs, Over all supervision. Vimal Manivannan. Chitra Karuppanan – Cell culture, Imaging and flow cytometer analysis. Dhinakarraj gopal and Raman Muthu samy- Study directors and manuscript corrections.

Funding Department of Biotechnology (DBT), New Delhi under the Translational Research Platform for Veterinary Biologicals, partnership program (DBT Sanction Number.102/IFD/DBT/SAN 2680/2011–2012) with TANUVAS, Chennai.

Data Availability The datasets used and/or analyzed during the current study are available from the corresponding author on reasonable request.

Declarations

Ethical Approval All in vivo studies were carried out in accordance with the instructions of the TANUVAS Ethical Committee, IAEC approval No.2172/ DFBS/2018 in Chennai.

Competing Interests The authors declare no competing interests.

References

1. Muller RH, Mader K, Gohla S (2000) Solid lipid nanoparticles (SLN) for controlled drug delivery - a review of the state of the art. Eur J Pharm Biopharm 50:161–177
2. Mukherjee S, Ray S, Thakur RS (2009) Solid lipid nanoparticles: a modern formulation approach in drug delivery system. Indian J Pharm Sci 71:349–358
3. Muller RH, Radtke M, Wissing SA (2002) Solid lipid nanoparticles (SLN) and nanostructured lipid carriers (NLC) in cosmetic and dermatological preparations. Adv Drug Deliv Rev 54:S131–S155
4. Wissing SA, Kayser O, Muller RH (2004) Solid lipid nanoparticles for parenteral drug delivery. Adv Drug Deliv Rev 56:1257–1272
5. Gal V, Runde M, Schuchmann HP (2016) Extending applications of high-pressure homogenization by using simultaneous emulsification and mixing (SEM)—an overview. Processes 4:1–15
6. Trotta M, Debernardi F, Caputo O (2003) Preparation of solid lipid nanoparticles by a solvent emulsification-diffusion technique. Int J Pharm 257:153–160
7. Soma D, Attari Z, Reddy MS, Damodaram A, Koteshwara KB (2017) Solid lipid nanoparticles of irbesartan: preparation, characterization, optimization and pharmacokinetic studies. Braz J Pharm Sci 53:e15012
8. Lander R, Manger W, Scouloudis M, Ku A, Davis C, Lee A (2000) Gaulin homogenization: a mechanistic study. Biotechnol Prog 16:80–85
9. Hu CMJ, Zhang L, Aryal S, Cheung C (2011) Erythrocyte membrane-camouflaged polymeric nanoparticles as a biomimetic delivery platform. PNAS 108:10980–10985
10. Parodi A, Quattrocchi N, van de Ven AL, Chiappini C, Evangelopoulos M, Martinez JO, Brown BS, Khaled SZ, Yazdi IK, Enzo MV, Isenhart L, Ferrari M, Tasciotti E (2013) Synthetic nanoparticles functionalized with biomimetic leukocyte membranes possess cell-like functions. Nat Nanotechnol 8:61–68
11. Fang RH, Hu CM, Luk BT, Gao W, Copp JA, Tai Y, O'Connor DE, Zhang L (2014) Cancer cell membrane-coated nanoparticles for anticancer vaccination and drug delivery. Nano Lett 14:2181–2188
12. Rothfield L, Pearlman-Kothencz M (1969) Synthesis and assembly of bacterial membrane components. A lipopolysaccharide-phospholipid-protein complex excreted by living bacteria. J Mol Biol 44:477–492
13. Osborn MJ, Wu HC (1980) Proteins of the outer membrane of gram-negative bacteria. Annu Rev Microbiol 34:369–422
14. Kobayashi.H, Ogawa M, Alford R, Choyke P L, Urano Y. (2010) New strategies for fluorescent probe design in medical diagnostic imaging. Chem Rev 110:2620–2640
15. Hassan M, Klaunberg BA (2004) Biomedical applications of fluorescence imaging in vivo. Comp Med 54:635–644
16. Resch-Genger.U, Grabolle M, Cavaliere-Jaricot S, Nitschke R, Nann T. (2008) Quantum dots versus organic dyes as fluorescent labels. Nat Methods 5:763–775
17. Jensen EC (2012) Use of Fluorescent Probes: Their Effect on Cell Biology and Limitations. Anat Rec 295:2031–2036
18. Yan J, Estévez MC, Smith JE, Wang K, He X, Wang L, Tan W (2007) Dye-doped nanoparticles for bioanalysis. Nano Today 2:44–50
19. Rampazzo E, Genovese D, Palomba F, Prodi L, Zaccheroni N (2018) NIR-fluorescent dye doped silica nanoparticles for in vivo imaging, sensing and theranostic. Methods Appl Fluoresc 6:022002
20. Song J, Qu J, Swihart MT, Prasad PN (2016) Near-IR responsive nanostructures for nanobiophotonics: emerging impacts on nanomedicine. Nanomedicine 12:771–788
21. Hemmer E, Venkatachalam N, Hyodo H, Hattori A, Ebina Y, Kishimoto H, Soga K (2013) Upconverting and NIR emitting rare earth based nanostructures for NIR-bioimaging. Nanoscale 5:11339–11346
22. Calderón-Colón X, Raimondi G, Benkoski JJ, Patrone JB (2015) Solid lipid nanoparticles (SLNs) for intracellular targeting applications. J Vis Exp 105:53102
23. Rostami E, Kashanian S, Azandaryani AH, Faramarzi H, Dolatabadi JE, Omidfar K (2014) Drug targeting using solid lipid nanoparticles. Chem Phys Lipids 181:56–61
24. Pardeshi C, Rajput P, Belgamwar V, Tekade A, Patil G, Chaudhary K, Sonje A (2012) Solid lipid based nanocarriers: an overview. Acta Pharm 62:433–472
25. Viswanathan K, Gopinath VP, Raj GD (2014) Formulation of Newcastle disease virus coupled calcium phosphate nanoparticles: an effective strategy for oculonasal delivery to chicken. Colloids Surf B Biointerfaces 116:9–16

Publisher's Note Springer Nature remains neutral with regard to jurisdictional claims in published maps and institutional affiliations.

Springer Nature or its licensor (e.g. a society or other partner) holds exclusive rights to this article under a publishing agreement with the author(s) or other rightsholder(s); author self-archiving of the accepted manuscript version of this article is solely governed by the terms of such publishing agreement and applicable law.